JACC: CARDIOVASCULAR IMAGING VOL. 4, NO. 12, 2011

ISSN 1936-878X/$36.00
PUBLISHED BY ELSEVIER INC. DOI:10.1016/j.jcmg.2011.06.023

Arterial Spin Labeled CMR Detects Clinically Relevant Increase in Myocardial Blood Flow With Vasodilation

Zungho Zun, PHD,* Padmini Varadarajan, MD,† Ramdas G. Pai, MD,†
Eric C. Wong, MD, PHD,‡ Krishna S. Nayak, PHD*
Los Angeles, Loma Linda, and La Jolla, California

OBJECTIVES This study sought to determine whether arterial spin labeled (ASL) cardiac magnetic resonance (CMR) is capable of detecting clinically relevant increases in regional myocardial blood flow (MBF) with vasodilator stress testing in human myocardium.

BACKGROUND Measurements of regional myocardial perfusion at rest and during vasodilatation are used to determine perfusion reserve, which indicates the presence and distribution of myocardial ischemia. ASL CMR is a perfusion imaging technique that does not require any contrast agents, and is therefore safe for use in patients with end-stage renal disease, and capable of repeated or continuous measurement.

METHODS Myocardial ASL scans at rest and during adenosine infusion were incorporated into a routine CMR adenosine induced vasodilator stress protocol and was performed in 29 patients. Patients who were suspected of having ischemic heart disease based on first-pass imaging also underwent x-ray angiography. Myocardial ASL was performed using double-gated flow-sensitive alternating inversion recovery tagging and balanced steady-state free precession imaging at 3-T.

RESULTS Sixteen patients were found to be normal and 13 patients were found to have visible perfusion defect based on first-pass CMR using intravenous gadolinium chelate. In the normal subjects, there was a statistically significant difference between MBF measured by ASL during adenosine infusion (3.67 ± 1.36 ml/g/min), compared to at rest (0.97 ± 0.64 ml/g/min), with $p < 0.0001$. There was also a statistically significant difference in perfusion reserve (MBF_{stress}/MBF_{rest}) between normal myocardial segments (3.18 ± 1.54) and the most ischemic segments in the patients with coronary artery disease identified by x-ray angiography (1.44 ± 0.97), with $p = 0.0011$.

CONCLUSIONS This study indicates that myocardial ASL is capable of detecting clinically relevant increases in MBF with vasodilatation and has the potential to identify myocardial ischemia. (J Am Coll Cardiol Img 2011;4:1253–61) © 2011 by the American College of Cardiology Foundation

From the *Ming Hsieh Department of Electrical Engineering, University of Southern California, Los Angeles, California; †Division of Cardiology, Loma Linda University Medical Center, Loma Linda, California; and the ‡Departments of Radiology and Psychiatry, University of California, San Diego, La Jolla, California. Dr. Wong has received research support from G.E. Healthcare. All other authors have reported that they have no relationships relevant to the contents of this paper to disclose.

Manuscript received March 5, 2010; revised manuscript received June 29, 2011, accepted June 30, 2011.

Assessment of myocardial perfusion, ventricular function, and coronary anatomy play important and complementary roles in the management of the patients with coronary artery disease (CAD). Myocardial perfusion imaging (MPI), when coupled with exercise, pharmacological stress, or vasodilation, indicates the presence and distribution of myocardial ischemia at rest and stress, and can demonstrate perfusion reserve. Myocardial perfusion refers here to the general phenomenon of blood delivery to the myocardium, and myocardial blood flow (MBF) refers to the rate of delivery, typically in ml (blood)/g (tissue)/min.

See page 1262

ABBREVIATIONS AND ACRONYMS

ASL = arterial spin labeling
CAD = coronary artery disease
CMR = cardiac magnetic resonance
ECG = electrocardiogram
ESRD = end-stage renal disease
FAIR = flow-sensitive alternating inversion recovery
MBF = myocardial blood flow
MPI = myocardial perfusion imaging
PET = positron emission tomography
SPECT = single-photon emission computed tomography
SSFP = steady-state free precession

There are several existing methods for MPI. Single-photon emission computed tomography (SPECT) is by far the most widely used approach, with 10 million scans performed each year. Positron emission tomography (PET) is an alternative that can quantify MBF. Both SPECT and PET have low spatial resolution and cannot reliably detect nontransmural perfusion deficits. In addition, exposure to ionizing radiation poses a risk to the patient and limits the use of these approaches for repeated or real-time scanning. Cardiac magnetic resonance (CMR) methods using contrast agents provide a means to qualitatively assess MBF, with higher spatial resolution and without the burden of radiation. In these methods, a bolus of intravenous contrast agent is administered, and the first pass of the bolus through the heart chambers and myocardium is monitored by rapid dynamic imaging. First-pass perfusion imaging is currently limited by unresolved artifacts (e.g., dark rim), difficulties with interobserver variability and absolute quantitation of MBF, and the toxic syndrome known as nephrogenic fibrosing dermopathy in patients with end-stage renal disease (ESRD) (1).

In this study, we evaluate a relatively new approach based on arterial spin labeling (ASL) CMR. Over the past few years, ASL CMR has become a powerful tool for the quantitative measurement of tissue blood flow. It is widely used in brain studies to measure regional cerebral blood flow (2) and has been applied successfully to perfusion measurement in other static tissues such as skeletal muscle (3) and kidneys (4). In ASL CMR, radiofrequency pulses are used to modify the longitudinal magnetization of arterial blood, generating an endogenous tag that decays away with a time constant given by the T1 relaxation time. After a delay to allow tagged blood to flow into the target tissue, an image is acquired that reflects the inflow of tagged blood as well as static tissue in the slice. A second (control) image is then acquired in the absence of a preceding tag pulse. The difference between these 2 images reflects the amount of tagged blood that has been delivered to the imaging region and, with appropriate tagging and imaging methods, can be made directly proportional to local tissue blood flow.

ASL techniques applied to myocardial perfusion have several potential advantages over contrast-based MPI methods. First, the ASL signal is directly proportional to tissue blood flow, and therefore quantitation of MBF should come more naturally. This method has the potential to reduce the problem of interobserver variability that affects qualitative first-pass MR perfusion imaging. Next, ASL does not require any contrast agents, resulting in reduced cost and reduced adverse effects. For example, ASL CMR could be safely applied in patients with ESRD who are not candidates for first-pass MPI. Finally, ASL can be performed continuously, which could open up new opportunities for repeated or even real-time monitoring of patients (e.g., before, during, and after interventions).

There has been preliminary work on myocardial ASL in humans (5–9). These preliminary studies have demonstrated the existence of an ASL signal in the heart, and while some have demonstrated signal increases with pharmacological stress, none has reported sufficient image quality and measurement consistency to provide useful diagnostic information in individual patients. We recently demonstrated a highly robust implementation of myocardial ASL based on double-gated flow-sensitive alternating inversion recovery (FAIR) tagging and balanced steady-state free precession (SSFP) imaging at 3-T (10). In healthy volunteers, we determined that MBF measurements at rest were consistent with ranges established by quantitative PET and that MBF measurements increased as expected with 2 forms of mild stress (passive leg elevation and isometric handgrip).

In this study, we applied myocardial ASL to the measurement of perfusion reserve in 29 patients scheduled for CMR. Data were collected at rest and during intravenous infusion of adenosine. We report the first perfusion reserve measurements with myocardial ASL that indicate that this method is

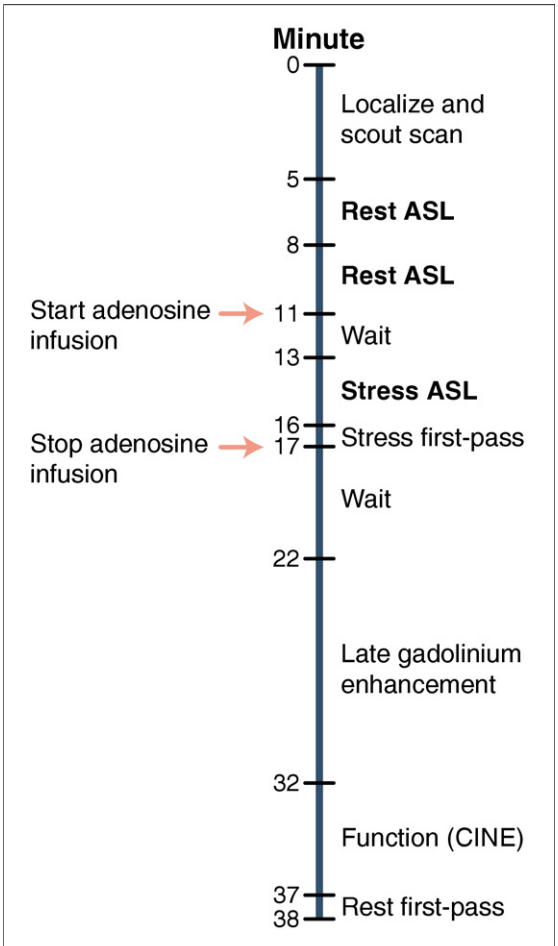

Figure 1. Modified Stress CMR Protocol

Myocardial arterial spin labeling (ASL) scans were performed at rest and during adenosine infusion, both before first-pass imaging to avoid confounding effects of the contrast agent (lowering the blood T1). The cardiac magnetic resonance (CMR) protocol after completion of adenosine infusion was unchanged and included viability and function imaging.

capable of detecting clinically relevant increases in MBF with vasodilation.

METHODS

Study design. Twenty-nine patients (age 64 ± 11 years; 19 women, 10 men) were recruited from among those suspected of having CAD and scheduled for stress CMR examinations at the Loma Linda University Heart and Imaging Center. This study was approved by our institutional review board, and each patient provided written informed consent.

Rest and stress myocardial ASL scans were incorporated into the routine CMR protocol as shown in Figure 1. All ASL scans were performed before first-pass perfusion imaging to prevent residual gadolinium from reducing the T1 of blood and confounding the computation of MBF from ASL images. Each ASL scan required 6 breath-holds and could be comfortably performed in 3 min. In most patients, 2 rest ASL scans were performed and averaged because the scan time was not limited at rest. The adenosine infusion was then started using the standard dosage (0.14 mg/kg/min). After 2 min, the stress ASL scan was performed. The average heart rates during rest and stress ASL scans were recorded independently. Immediately after the stress ASL scan, CMR first-pass perfusion was performed between min 5 and 6 of the adenosine infusion (total infusion duration = 6 min). During the infusion, the medical status of the patient was monitored by a nurse, and the patient was asked frequently if he or she felt any adverse symptoms of adenosine. The rest of the CMR imaging protocol remained unchanged, and included late gadolinium enhancement and cardiac function cinema/video (CINE) imaging. Based on the CMR results, patients who were suspected of having severe ischemic heart disease also underwent x-ray coronary angiography within 1 month.

Imaging methods. Myocardial ASL was performed at a single mid–short-axis slice using FAIR tagging and balanced SSFP imaging (10). Tagging was achieved by applying nonselective and selective adiabatic inversions. Imaging was performed with snap-shot 2-dimensional Fourier transform SSFP acquisition with repetition time (TR) of 3.2 ms (total duration = 313 ms), flip-angle of 50°, matrix size of 96 × 96 over a 24- to 32-cm isotropic field of view, full k-space acquisition, and slice thickness of 1 cm. Parallel imaging was not used. Both tagging and imaging were performed at mid-diastole using electrocardiogram (ECG) gating. The trigger delay was determined from a CINE scout scan. Each ASL scan required 6 breath-holds, with 1 pair of tagged and control images acquired in each breath-hold. Each breath-hold lasted 10 s, and the total scan time was 3 min (including breaks). The myocardial ASL pulse sequence is fully described by Zun et al. (10).

The routine CMR first-pass perfusion sequence covered 4 short-axis slices using a saturation recovery fast gradient echo pulse sequence. The imaging parameters were: TR of 6.5 ms, flip-angle of 10°, matrix size of 128 × 128, and slice thickness of 1 cm. The intravascular contrast-agent (Gd-BOPTA, [MultiHance, Bracco Diagnostics Inc., Milan, Italy]; dosage 0.05 mmol/kg) and saline flush (20 ml) was injected at a rate of 5 ml/s. The total scan

time was 54 s, and the subjects were instructed to hold their breath as long as possible and then initiate shallow breathing.

All CMR experiments were performed on a GE Signa 3.0 T EXCITE HDx system (GE Healthcare, Waukesha, Wisconsin) with gradients supporting 40 mT/m amplitude and 150 mT/m/ms slew rate. The body coil and an 8-channel cardiac array coil were used for radiofrequency transmission and signal reception, respectively. Coronary angiography was performed using the standard techniques, and tomographic images were obtained from multiple planes.

Image analysis. Endocardial and epicardial borders of the left ventricle were manually drawn for each tagged and control image. For segment-based analysis, the myocardium was divided into 6 radial segments (anterior, anteroseptal, inferoseptal, inferior, inferolateral, and anterolateral) (11), and MBF was calculated using a modified version of Buxton's general kinetic model (12) after signal averaging in each segment. The SD of the physiological noise affecting each scan was estimated using 6 associated measurements (1 per breath-hold). Perfusion reserve was computed as MBF_{stress}/MBF_{rest}. To generate perfusion reserve maps, each MBF map was reconstructed with 50 radial segments and then smoothed by convolving with a 13-point Hamming window.

CMR first-pass images and x-ray angiograms were read by 2 experienced cardiologists. For first-pass images, all 6 myocardial segments from 4 slices were examined for perfusion defects. Patients were classified as "normal" if having no visible perfusion defect on first-pass CMR, and the other patients were classified as having perfusion defect. In x-ray angiography, coronary artery narrowing was visually estimated using electronic calipers, and significant stenosis was defined as >70% diameter narrowing. In each patient with perfusion defect, the most ischemic segments were determined by the most significant lesion on the angiograms.

Statistical analysis. From the cardiac ASL data, we computed global MBF on the basis of all pixels in the slice containing left ventricular myocardium, and calculated segmental MBF and MBF reserve for each myocardial segment within the slice. In the normal subjects, we compared the measured global MBF at rest and during stress using a Student paired *t* test. We also compared the measured segmental MBF reserve in normal segments and the most ischemic segments using a mixed-effects model, taking into account the correlation among segmental measurements from the same subjects.

Table 1. Comparison Between Normal Myocardial Segments From Normal Patients and the Most Ischemic Myocardial Segments From Patients With Perfusion Defect

	Normal Segments	Ischemic Segments
Subjects		
n	16	13
Age, yrs	64 ± 12	64 ± 11
Sex		
Male	3	7
Female	13	6
Risk factors		
Hypertension	15	12
Hypercholesterolemia	10	11
Age older than 65 yrs	8	7
Diabetes mellitus	5	7
Male	3	7
Indications		
Chest pain	9	11
Pre-operative workup	6	3
Shortness of breath	3	4
Abnormal echocardiogram	2	2
Abnormal ECG	2	0
Significant coronary lesions	None	7 RCA, 4 LAD, 2 LCX
Segments		
No. of segments included	59	11
Perfusion reserve (MBF_{stress}/MBF_{rest})	3.18 ± 1.54*	1.44 ± 0.97*

Values are n or mean ± SD. *The difference in perfusion reserve between normal and ischemic segments was statistically significant (p = 0.0011) on the basis of a mixed-effects model.
ECG = electrocardiogram; LAD = left anterior descending; LCX = left circumflex (artery); MBF = myocardial blood flow; RCA = right coronary artery.

RESULTS

Patient classification. Among the 29 patients, the mean number of risk factors was 3.4, with 97% hypertension, 72% hypercholesterolemia, 52% age older than 65 years, 41% diabetes mellitus, and 34% male. Indications that led to CMR examination included 69% chest pain, 31% preoperative workup, 24% shortness of breath, 14% abnormal echocardiogram, and 7% abnormal ECG. Sixteen of the 29 patients were found to be "normal," and the other 13 patients had perfusion defect (Table 1).

Global MBF in normal patients. Figure 2 contains global MBF measurements based on ASL at rest and stress from the 16 normal subjects. Each bar represents the average MBF across the whole myocardium in the slice. The error bars correspond to ±1 SD of the physiological noise, σ measured for each scan. The MBF across subjects was 0.97 ±

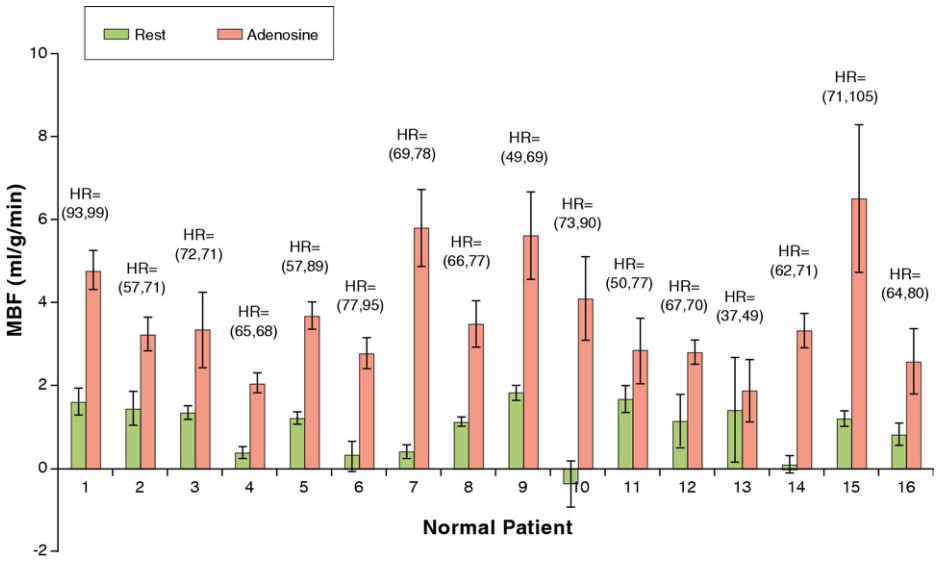

Figure 2. Global MBF Estimates at Rest and During Stress

Global myocardial blood flow (MBF) was measured at rest **(green)** and during adenosine infusion **(pink)** in 16 patients with no significant perfusion defect on first-pass imaging. The MBF was 0.97 ± 0.64 ml/g/min at rest and 3.67 ± 1.36 ml/g/min with adenosine, yielding an average perfusion reserve (MBF_{stress}/MBF_{rest}) of 3.94. This increase in MBF was found to be statistically significant based on the Student paired *t* test ($p < 0.0001$). Error bars represent ±1 SD of the measured physiological noise. The average physiological noise during adenosine infusion was 2.1 times larger than the average physiological noise at rest. HR = heart rate.

0.64 ml/g/min at rest and 3.67 ± 1.36 ml/g/min during adenosine infusion, yielding an average perfusion reserve (MBF_{stress}/MBF_{rest}) of 3.94. Subjects with $MBF_{rest}/\sigma_{rest} < 1.0$ were excluded from perfusion reserve analysis because excessive noise in the denominator of the perfusion reserve equation can produce substantive errors in the estimated perfusion reserve. This resulted in exclusion of Patients #6, #10, and #14 in Figure 2 from the reserve estimation.

On the basis of a Student paired *t* test, the MBF increase with adenosine was found to be statistically significant ($p < 0.0001$). The average SD of physiological noise across subjects for the rest ASL scans was 0.34 ml/g/min. The average SD of physiological noise for the stress ASL scans was 0.70 ml/g/min, which is roughly 2.1 times larger than that of the physiological noise at rest. The average heart rate increased by 23% from 64 beats/min at rest to 79 beats/min during adenosine infusion.

Segmental reserve and detection of disease. Table 1 summarizes the comparison between normal myocardial segments from the 16 normal patients and the most ischemic myocardial segments from the 13 patients with abnormal first-pass perfusion. All 6 mid–short-axis segments (11) were included for the normal patients. Ischemic segments included the most ischemic segments in each patient with abnormal perfusion. Two patients among 13 with perfusion defect showed no significant stenosis identified by using x-ray angiography. Segments with $MBF_{rest}/\sigma_{rest} < 2.0$ were excluded for the same reasons mentioned here. The average perfusion reserve was 3.18 ± 1.54 in normal segments and 1.44 ± 0.97 in ischemic segments. This difference in perfusion reserve was found to be statistically significant ($p = 0.0011$) based on a mixed-effects model.

Figure 3 shows segment-based MBF at rest and during adenosine infusion for 11 normal segments randomly selected out of 59 and for all 11 ischemic segments. The ischemic segments are named and annotated with the name of the coronary branch(es) that exhibited the most significant stenosis on angiography.

Perfusion reserve maps. Figure 4 contains perfusion reserve maps and coronary angiograms from 2 representative patients with single-vessel disease. Lowered perfusion reserve in the anterior wall from the first patient is consistent with total occlusion of the left anterior descending coronary artery, and lowered perfusion reserve in the inferoseptum from the second patient is consistent with total occlusion of the right coronary artery (RCA). The inferior wall in the first patient and the lateral wall in the

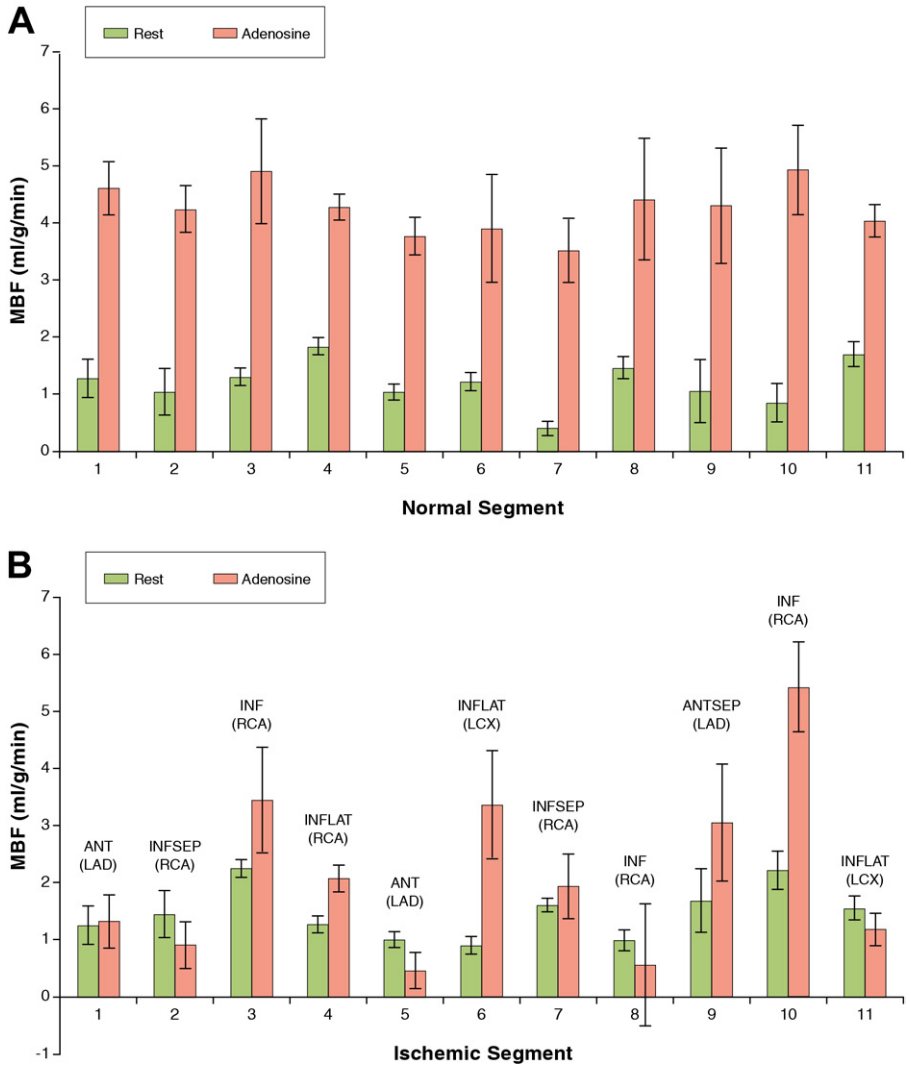

Figure 3. Segmental MBF Estimates at Rest and During Stress

Segmental MBF was measured at rest **(green)** and during adenosine infusion **(pink)** in **A** 11 normal segments randomly selected out of 59 and in **B** all 11 ischemic segments from Table 1 (segments in arbitrary order). Ischemic segments are annotated with the segment name and the most diseased coronary branch on angiography in that patient. The difference in perfusion reserve between normal and ischemic segments was statistically significant. LAD = left anterior descending; LCX = left circumflex artery; RCA = right coronary artery; other abbreviations as in Figure 2.

second patient also showed somewhat lowered reserve, and it is not clear from the angiogram whether these reflect real perfusion deficit or merely measurement error due to high noise.

DISCUSSION

In this study, we applied myocardial ASL sequences to 29 patients scheduled for rest and stress CMR. In patients who had no visible myocardial perfusion defect on first-pass imaging, we found a statistically significant increase in global MBF measurements with adenosine infusion (3.67 ± 1.36 ml/g/min) compared with at rest (0.97 ± 0.64 ml/g/min). This finding demonstrates that myocardial ASL is able to detect a clinically relevant increase in MBF with vasodilation. We also found a statistically significant difference in measured perfusion reserve between normal myocardial segments and the most ischemic myocardial segments identified by x-ray angiography in patients with abnormal first-pass perfusion, suggesting the potential for rest and stress myocardial ASL to detect angiographically significant CAD.

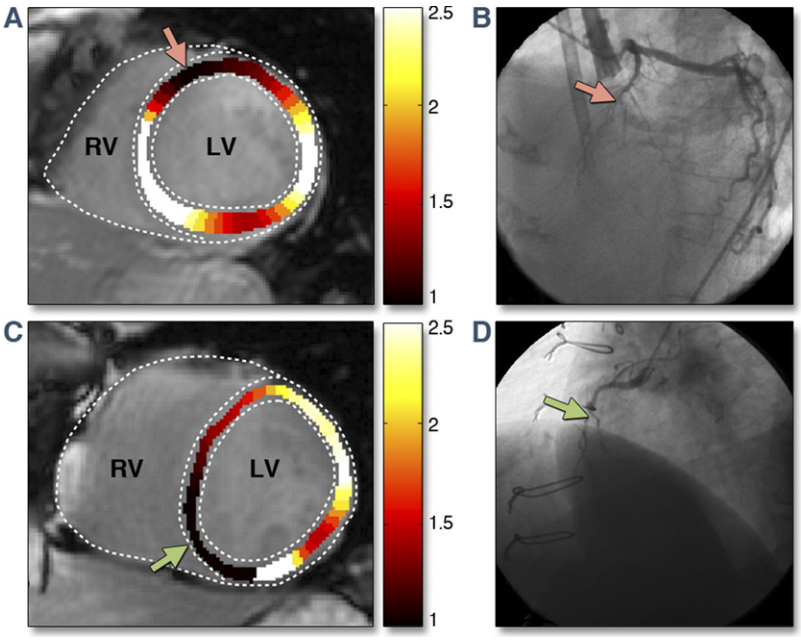

Figure 4. ASL Perfusion Reserve Maps and X-Ray Angiograms From 2 Patients

(A, B) Patient with total left anterior descending occlusion; **(C, D)** patient with total right coronary artery occlusion. Myocardial regions with lowered perfusion reserve were consistent with the territories of occluded vessels **(arrows)**. The **pink** and **green arrows** correspond to ischemic segments 1 and 2 in Figure 3B, respectively. LV = left ventricle; RV = right ventricle; other abbreviation as in Figure 1.

Perfusion reserve begins to decrease earlier than resting MBF with onset of stenosis and is a useful index for the detection of CAD (13). Using adenosine, perfusion reserve in normal myocardium has been documented to be 4.00 ± 1.10 (14), 4.23 ± 1.29 (15), 2.54 ± 0.92 (16), and 2.24 ± 0.55 (17) with PET, and 3.69 ± 2.79 (18) with SPECT. Our measurements of perfusion reserve in normal patients (3.94 ± 3.41) is comparable to these published literature values while showing larger variance due to high physiological noise.

Spatial heterogeneity of MBF has been observed in humans and animals (19–23) and may be attributed to different metabolic needs, oxygen demand, and neural regulatory modification in different regions (19,21,22). It is typically represented by a unitless metric called relative dispersion (SD/mean). MBF relative dispersion has been reported to be 0.13 with 4 segments of myocardium (anterior, lateral, septal, and inferior walls) using PET in normal humans (23) and 0.26 with 8 segments of myocardium using microspheres in normal baboons (20). In this study, the relative dispersion of measured MBF from normal patients at rest was 0.68 (range 0.11 to 1.52) with 6 myocardial segments. This value is larger than that reported with other modalities, likely due to the higher level of physiological noise in myocardial ASL (10).

An important follow-up study would be to compare ASL measurements against an independent gold standard measure of MBF in humans, such as quantitative PET. In this work, we invoked the widely used general kinetic model (12) to convert ASL signal amplitudes to MBF estimates. Although it is known that ASL signal amplitude is proportional to tissue blood flow, there are several other factors that may influence the quantitative accuracy of the approach, including transit delays, water exchange rates, and the difference in T1 relaxation time between blood and myocardium.

Current implementations of myocardial ASL (9,10), including the one used in this work, suffer from greater noise and lower spatial resolution compared with state-of-the-art first-pass imaging. These are not fundamental limitations of the ASL approach and are likely to improve with technical developments such as the incorporation of highly selective tagging and background suppression, which have been used successfully in brain ASL (24,25) and are currently under investigation for myocardial ASL (26,27). Even in its present form, myocardial ASL could be of value in evaluating

patients with ESRD who are not candidates for first-pass imaging due to the risk of nephrogenic fibrosing dermopathy. There are roughly 340,000 patients with ESRD in the United States (28) who require heart disease assessment every 6 to 12 months while awaiting kidney transplant, and most patients are on the wait-list for 4 to 7 years. These patients stand to benefit significantly from a new MPI approach that does not require contrast agents.

Study limitations. We have previously found that physiological noise (which includes all variations over time) is the critical factor that determines the sensitivity of ASL to MBF (10). Patient #10 (Fig. 2) represents one of the worst cases; this patient experienced physiological noise 2× higher than the subject average, which resulted in a negative resting MBF measurement. Sources of physiological noise may include metabolic fluctuation, respiratory and cardiac motion, and subject discomfort. The fact that physiological noise was 2.1× larger during adenosine infusion suggests that subject motion or discomfort may be a significant source. Myocardial ASL also requires signal averaging spatially and over multiple repetitions to generate meaningful data. This results in lower resolution but is expected to improve with technical development, including the reduction of physiological noise. Finally, the current implementation images a single mid–short-axis slice, which is insufficient for routine clinical use. This approach, however, can be repeated to cover multiple slices or extended to acquire multiple slices simultaneously with the same signal-to-noise ratio and no additional scan time, by using parallel imaging.

CONCLUSIONS

This study demonstrated that myocardial ASL CMR is capable of detecting clinically relevant increases in MBF with vasodilation and has the potential to identify myocardial ischemia. This may provide an alternative perfusion method to assess patients who are not candidates for first-pass imaging, such as those with ESRD.

Reprint requests and correspondence: Dr. Krishna S. Nayak, 3740 McClintock Avenue, EEB 406, University of Southern California, Los Angeles, California 90089-2564. *E-mail: knayak@usc.edu.*

REFERENCES

1. Sieber MA, Lengsfeld P, Walter J, et al. Gadolinium-based contrast agents and their potential role in the pathogenesis of nephrogenic systemic fibrosis: the role of excess ligand. J Magn Reson Imaging 2008;27:955–62.
2. Detre JA, Wang J, Wang Z, Rao H. Arterial spin-labeled perfusion MRI in basic and clinical neuroscience. Curr Opin Neurol 2009;22:348–55.
3. Wu WC, Mohler E III, Ratcliffe SJ, Wehrli FW, Detre JA, Floyd TF. Skeletal muscle microvascular flow in progressive peripheral artery disease: assessment with continuous arterial spin-labeling perfusion magnetic resonance imaging. J Am Coll Cardiol 2009;53:2372–7.
4. Fenchel M, Martirosian P, Langanke J, et al. Perfusion MR imaging with FAIR true FISP spin labeling in patients with and without renal artery stenosis: initial experience. Radiology 2006;238:1013–21.
5. Poncelet BP, Koelling TM, Schmidt CJ, et al. Measurement of human myocardial perfusion by double-gated flow alternating inversion recovery EPI. Magn Reson Med 1999;41:510–9.
6. Wacker CM, Fidler F, Dueren C, et al. Quantitative assessment of myocardial perfusion with a spin-labeling technique: preliminary results in patients with coronary artery disease. J Magn Reson Imaging 2003;18:555–60.
7. Zhang H, Shea SM, Park V, et al. Accurate myocardial T1 measurements: toward quantification of myocardial blood flow with arterial spin labeling. Magn Reson Med 2005;53:1135–42.
8. Northrup BE, McCommis KS, Zhang H, et al. Resting myocardial perfusion quantification with CMR arterial spin labeling at 1.5 T and 3.0 T. J Cardiovasc Magn Reson 2008;10:53.
9. Wang DJ, Bi X, Avants BB, Meng T, Zuehlsdorff S, Detre JA. Estimation of perfusion and arterial transit time in myocardium using free-breathing myocardial arterial spin labeling with navigator-echo. Magn Reson Med 2010;64:1289–95.
10. Zun Z, Wong EC, Nayak KS. Assessment of myocardial blood flow (MBF) in humans using arterial spin labeling (ASL): feasibility and noise analysis. Magn Reson Med 2009;62:975–83.
11. Cerqueira MD, Weissman NJ, Dilsizian V, et al. Standardized myocardial segmentation and nomenclature for tomographic imaging of the heart: a statement for healthcare professionals from the Cardiac Imaging Committee of the Council On Clinical Cardiology of the American Heart Association. Circulation 2002;105:539–42.
12. Buxton RB, Frank LR, Wong EC, Siewert B, Warach S, Edelman RR. A general kinetic model for quantitative perfusion imaging with arterial spin labeling. Magn Reson Med 1998;40:383–96.
13. Gould KL, Lipscomb K. Effects on coronary stenoses on coronary flow reserve and resistance. Am J Cardiol 1974;34:48–55.
14. Kaufmann PA, Rimoldi OE, Gnecchi-Ruscone T, Luscher TF, Camici PG. Systemic nitric oxide synthase inhibition improves coronary flow reserve to adenosine in patients with significant stenoses. Am J Physiol Heart Circ Physiol 2007;293:H2178–82.
15. Kaufmann PA, Gnecchi-Ruscone T, Schäfers KP, Lüscher TF, Camici PG. Low density lipoprotein cholesterol and coronary microvascular dysfunction in hypercholesterolemia. J Am Coll Cardiol 2000;36:103–9.
16. Wu YW, Chen YH, Wang SS, et al. PET assessment of myocardial perfusion reserve inversely correlates with intravascular ultrasound findings in angiographically normal cardiac transplant recipients. J Nucl Med 2010;51:906–12.

17. Knesaurek K, Machac J, Zhang Z. Repeatability of regional myocardial blood flow calculation in 82Rb PET imaging. BMC Med Phys 2009;9:2.
18. Abdelmoneim SS, Dhoble A, Bernier M, et al. Absolute myocardial blood flow determination using real-time myocardial contrast echocardiography during adenosine stress: comparison with single-photon emission computed tomography. Heart 2009;95:1662–8.
19. Marcus ML, Kerber RE, Erhardt JC, et al. Spatial and temporal heterogeneity of left ventricular perfusion in awake dogs. Am Heart J 1977;94:748–54.
20. King R, Bassingthwaighte J, Hales J, Rowell L. Stability of heterogeneity of myocardial blood flow in normal awake baboons. Circ Res 1985;57:285–95.
21. Hoffman JIE. Heterogeneity of myocardial blood flow. Basic Res Cardiol 1995;90:103–11.
22. Deussen A. Blood flow heterogeneity in the heart. Basic Res Cardiol 1998;93:430–38.
23. Chareonthaitawee P, Kaufmann PA, Rimoldi O, Camici PG. Heterogeneity of resting and hyperemic myocardial blood flow in healthy humans. Cardiovasc Res 2001;50:151–61.
24. Wong EC, Cronin M, Wu WC, Inglis B, Frank LR, Liu TT. Velocity-selective arterial spin labeling. Magn Reson Med 2006;55:1334–41.
25. Wong EC. Vessel-encoded arterial spin-labeling using pseudocontinuous tagging. Magn Reson Med 2007;58:1086–91.
26. Zun Z, Wong EC, Nayak KS. Arterial spin labeled myocardial perfusion imaging with background suppression. Proceedings of the 16th Annual Meeting of ISMRM. Toronto, Canada: International Society for Magnetic Resonance in Medicine, 2008:997.
27. Zun Z, Wong EC, Nayak KS. Background Suppression Does Not Reduce Physiological Noise in Myocardial ASL Perfusion Imaging. In: Proceedings of the 17th Annual Meeting of ISMRM. Honolulu, HI: International Society for Magnetic Resonance in Medicine, 2009:1735.
28. United States Renal Data System, 2009 annual data report. Available at: http://www.usrds.org/atlas.aspx. Accessed March 1, 2010.

Key Words: adenosine ■ arterial spin labeling ■ cardiac magnetic resonance ■ myocardial blood flow ■ perfusion.